How to cite: *Angew. Chem. Int. Ed.* **2022,** *61,* e202201577
International Edition: doi.org/10.1002/anie.202201577
German Edition: doi.org/10.1002/ange.202201577

VIP **Phthalocyanines** **Very Important Paper**

# Triggering near-infrared luminescence of vanadyl phthalocyanine by charging

*Sreekanta Debnath, Karolina A. Haupa,* Sergei Lebedkin, Dmitry Strelnikov, and Manfred M. Kappes**

**Abstract:** Probing electrofluorochromism (EFC) at the molecular level remains challenging. Here we study the strongly charge state-dependent photoluminescence of vanadyl phthalocyanine. We report vibrationally resolved absorption and laser-induced fluorescence (LIF) spectra of samples comprising both the mass-selected neutral molecule ($VOPc^{\bullet}$, a stable radical) and its cation produced upon electron ionization (EI) isolated in 5 K neon matrices. Ionization of the essentially non-emissive $VOPc^{\bullet}$ forms a high-spin diradical cation ($VOPc^{+\bullet\bullet}$) which shows profound photoluminescence (PL) in the NIR range. This unique phenomenon is potentially of interest for NIR-emitting electro-optic devices.

## Introduction

The luminescence properties of numerous molecules are stimuli-responsive. Among them, electrofluorochromism, i.e. dependence of luminescence on charge state, is of particular interest due to its wide range of potential technological applications.[1] One such application is "on-off" fluorescence switching[2] in which molecules typically cycle between emissive closed-shell neutral and non-emissive radical-ion charge states. Strongly luminescent radical-ions are unusual due to competition from other relaxation channels.[1a,3] Furthermore, probing EFC at the molecular level remains challenging owing to the limitations of state-of-art methods and correspondingly the fundamentals remain poorly investigated.

Nevertheless, there have been some reports of prominent emissions from radical cations.[1a,4] Among them are mono- and diradicals[5] with the same overall molecular framework but different delocalization of both spin and charge - leading to contrasting luminescent properties. Bill et al. have for example reported that sequential one-electron oxidation of π-extended tetrathiafulvalene BODIPY (ex-TTF-BODIPY) to its mono- and diradical ions are associated with "on-off-on" electro-switchable fluorescence in the NIR spectral region.[6] In a related study, Namai et al. have shown that trimethylenemethane (TMM) derivatives, known to form high-spin diradicals, can be used in OLEDs where they emit via triplet-triplet fluorescence in a process also involving (dark) TMM monoradical cations.[7] In this contribution, we report charge state dependent NIR-range photoluminescence of vanadyl phthalocyanine, a commonly available member of the phthalocyanine (Pc) chromophore family.

Free-base Pc′s, their metal complexes and derivatives have long been recognized for their photostability, high fluorescence quantum yields, strong absorption in the 550–750 nm range, and respective long-wavelength emission maxima up to the NIR region. Their promising optical and electrical properties have been exploited in various applications including optoelectronics.[8] Although the optical properties of free-base and metallized Pc′s are well characterized in neutral form, much less is known about the corresponding ions. This reflects the inherent difficulty of preparing well-defined samples of molecular ions for spectroscopy. However, this situation is now rapidly improving owing to various recent methodological advances. For example, light emission scanning tunneling microscopy methods (LE-STM) have allowed measuring charge-state-dependent photoluminescence properties of metallo-phthalocyanines at the single-molecule level. Rai *et al.* found, that the intensity of light emitted from a single free-base phthalocyanine ($H_2Pc$) adsorbed onto an insulating surface can be boosted by a factor of 19 upon charging.[9] Similarly, Doppagne *et al.* used LE-STM to observe enhanced light emission from single Zn-phthalocyanine (ZnPc) molecules upon ionization.[10] We have recently shown, that inert gas matrix isolation spectroscopy at cryogenic temperatures provides complementary information to explore the electrofluorochromic behavior of ZnPc and $H_2Pc$ in the absence of STM-tip and surface-induced perturbations.[11] Specifically, mass-selective, low energy ion beam deposition into Ne

[*] Dr. S. Debnath, Dr. K. A. Haupa, Dr. D. Strelnikov, Prof. Dr. M. M. Kappes
Institute of Physical Chemistry II,
Karlsruhe Institute of Technology
Fritz-Haber-Weg 2, 76131 Karlsruhe (Germany)
E-mail: karolina.haupa@gmail.com
manfred.kappes@kit.edu
Dr. S. Lebedkin, Prof. Dr. M. M. Kappes
Institute of Nanotechnology,
Karlsruhe Institute of Technology
Hermann-von-Helmholtz-Platz 1, 76344 Eggenstein-Leopoldshafen (Germany)



 

matrix allowed to obtain vibrationally resolved electronic absorption and emission spectra of the isolated molecules in several charge states.[12] Here, we have used the same approach in combination with theory to study vanadyl phthalocyanine and its cation in solid Ne at 5 K.

Vanadyl phthalocyanine (VOPc•), a stable monoradical (doublet spin state) is a unique representative of the Pc class. It features a pyramidal structure with the unpaired electron localized mainly on the central $[V{=}O]^{2+}$ and interacting weakly with the four pyrrolic N-atoms—as inferred from the ESR study.[13] Although many properties of neutral VOPc• have been well characterized, there are only a few literature available photoluminescence studies—in solution and solid-state.[13–15] To the best of our knowledge, no spectroscopic reports on VOPc cations have yet been published.

## Results and Discussion

DFT calculations at the (TD)-B3LYP/cc-pVDZ level predict that upon ionization VOPc• can form two different spin-isomers: anti-ferromagnetically coupled singlet ($VOPc^+$) and ferromagnetically coupled triplet ($VOPc^{+\bullet\bullet}$). The optimized geometry of $VOPc^{+\bullet\bullet}$ ($C_{4v}$, pyramidal) is similar to that of the neutral, whereas $VOPc^+$ is predicted to have a different $C_{2v}$ symmetric "blender knife" structure (see Figure 1a). This significant structural difference is associated with a destabilization of $VOPc^+$ relative to $VOPc^{+\bullet\bullet}$ by 73 kJ mol$^{-1}$. Figure 1b illustrates the Jablonski diagram of possible photophysical events for VOPc•, $VOPc^+$, and $VOPc^{+\bullet\bullet}$. The observed absorption and fluorescence processes (and their assignments) are indicated in green and pink, respectively. Figures S6–S8, show the corresponding frontier molecular orbital geometries, their energy levels, and electron occupancies for VOPc•, $VOPc^+$, and $VOPc^{+\bullet\bullet}$, respectively.

VOPc cations were produced in an electron-impact ionization source (70 eV), transferred via Einzel lenses, mass-selected with a quadrupole mass filter, and soft-landed with an excess of co-deposited Ne gas onto an Al-on-quartz mirror cooled to 5 K (see the methods section in Supporting Information for details). In contrast to light emission scanning tunneling microscopy (LE-STM) measurements,[16] we did not observe the loss of oxygen from VOPc• under our ionization conditions (Figure S3). This makes us confident that the as-deposited ions remain stable during the subsequent acquisition of absorption and LIF spectra. Note, however, that deposition of only positively charged ions into an insulating matrix results in charge accumulation. Hence, the charge must be partially compensated to prevent further incoming ions from being deflected away. We accomplished this by adding electron scavengers ($SF_6$ and $CHCl_3$) to the matrix. They capture electrons from the surroundings and produce anions ($\bar{e} + CH_3Cl \rightarrow CH_3^\bullet + Cl^-$). This prevents discharges from conductive mirror substrate to the matrix and minimizes neutralization of trapped cations, as well as compensates for the charge. Thus, it enhances the cation to neutral ratio in the matrix.[17]

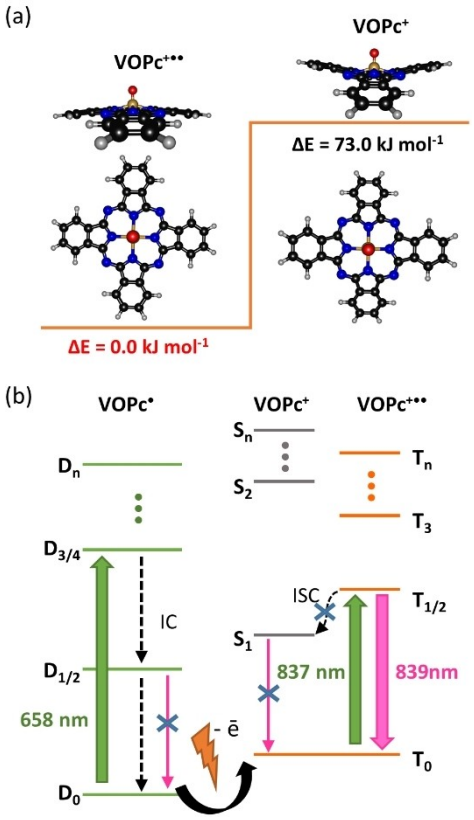


***Figure 1.*** a) Two lowest energy isomers of cationic VOPc calculated at the (TD)-B3LYP/cc-pVDZ level (top and side view). b) Jablonski diagram showing the possible photophysical processes that can occur in neutral and cationic VOPc; green and pink arrows indicate the assignments of observed absorptions and emissions, respectively. IC = internal conversion, ISC = intersystem crossing.

The top panel of Figure 2 represents the experimental absorption spectrum of mass-selected VOPc cations deposited into the Ne matrix and measured in the UV/Vis-NIR region. It is compared to the spectra of matrices with added $SF_6$ and $CHCl_3$ scavengers (bottom two panels). Two groups of well-resolved intense bands can be observed in all three spectra. The higher energy band at 658 nm shows a clearly distinguishable vibrational progression (with its two most intense features at 628 and 596 nm). The lower energy band at 837 nm shows a weaker vibronic structure. Broad multi-structured Soret band(s) can be observed from 275 to 400 nm. In the presence of scavengers, the relative intensity of the 837 nm peak is enhanced. Thus, we assign this peak to the (incident) cationic charge state and the peak at 658 nm to *neutralized* VOPc.[11] The experimental peak positions are consistent with the vertical excitations calculated using the (TD)-B3LYP/cc-pvDZ method (see Table S2). The first doubly degenerated (vertical) electronic transition ($D_0 \rightarrow D_{1/2}$) calculated for VOPc• is predicted at 1150 nm. It is predicted to have zero oscillator strength. (Note, that analogous electronic phenomena are responsible for the absence of luminescence from a low-lying dark state in CuPc).[18] By contrast, the vertical electronic transition to $D_{3/4}$ predicted for VOPc• at 618 nm (experiment: 658 nm)

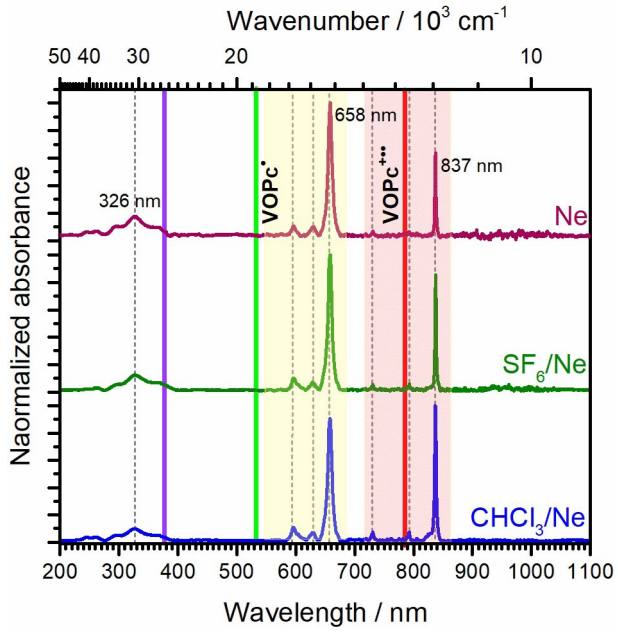


***Figure 2.*** UV/Vis-NIR absorption spectra obtained upon depositing cationic VOPc into Ne matrix at 5 K (top panel). Assignments and positions of the main spectral features are indicated. Spectral features in the yellow and pink shaded regions are assigned as the signatures of $VOPc^{\bullet}$ and $VOPc^{+\bullet\bullet}$ respectively. Note the presence of both neutralized and cationic VOPc in the same matrix. Electron scavengers $SF_6$ and $CHCl_3$ were used to enhance the relative concentration of the cationic species w.r.t the neutrals (bottom panels). Dashed gray lines highlight the positions of absorption bands common to all three spectra. Purple, green, and red lines denote the central wavelengths of laser diodes used for LIF (see text).

with an oscillator strength of $f=0.37$ is fully allowed. Huang and Sharp reported that the absorption spectrum of neutral VOPc in α-chloronapthalene solution has a band maximum at 701 nm.[15] A corresponding 43 nm red-shift relative to the absorption maximum in the Ne matrix is plausible considering solvatochromic effects.[19]

The first excited electronic state of $VOPc^+$ is predicted at 1102 nm (*vertical excitation* with oscillator strength $f=2.5\times10^{-3}$), followed by two transitions with relatively large oscillator strengths predicted at 720 ($f=0.13$) and 657 nm ($f=0.18$). However, there is no evidence for these two transitions (which should show fixed intensity ratio) and therefore for the presence of this species in our matrix spectra. Instead, the TD-DFT calculations imply that ionization leads to $VOPc^{+\bullet\bullet}$: the first doubly degenerate $T_0\rightarrow T_1$ transition[1] is predicted at 783 nm with oscillator strength $f=0.07$. The strong absorption in the experimental spectrum at 837 nm with vibronic structure extending to 700 nm satisfactorily agrees with this prediction.

To better understand the spectral pattern and derive assignments, simulations of *vibrationally-resolved absorption spectra* with Franck–Condon (FC) and combined Franck–Condon–Herzberg–Teller (FCHT) approximations were also performed. The optimized geometry of $VOPc^{+\bullet\bullet}$ in its $T_1$ state is presented in Figure S9. Furthermore, a comparison of the observed to the predicted spectra is presented in Figure S10 and listed in Table S3. When considering optimized structures and normal-mode analysis of the ground and the first excited states of $VOPc^{+\bullet\bullet}$, the $T_0\rightarrow T_1$ band origin is predicted at 11803 $cm^{-1}$ (847 nm) with a deviation of only 1.24 % from the observed line at 11950 $cm^{-1}$ (837 nm). (Note, that the significant red-shift relative to the (vibrationless) vertical excitation listed in the previous paragraph derives from generally somewhat softer vibrational modes in the upper state). The experimental vibronic structure is relatively weak and cannot be fully reproduced by the theory. However, significant similarities between the predicted and observed spectral patterns can be noticed as illustrated in Figure S10. Given that TD-DFT is known to be less successful at describing comparable open-shell systems, we regard the overall level of agreement as satisfactory and in support of our assignments (see Table S3).

The LIF spectrum of $VOPc^{+\bullet\bullet}$ recorded with 532 nm excitation is presented in Figure 3. A strong emission with its maximum at 11923 $cm^{-1}$ (839 nm) and associated vibrational structure has been observed. The same emission pattern was also seen for the two other excitation wavelengths used, following Kasha's rule,[20] as shown in Figure S11. Full FCHT simulations including the geometry optimized first excited $T_1$ state are in good agreement with the observed LIF emission pattern (Figure 3). Thereby, the assignment of $VOPc^{+\bullet\bullet}$ as the carrier of the characteristic vibrationally resolved absorption and emission features is strongly supported.

It can also be seen from Figure 3, that inclusion of the Herzberg–Teller (HT) effect within the Frank–Condon (FC)

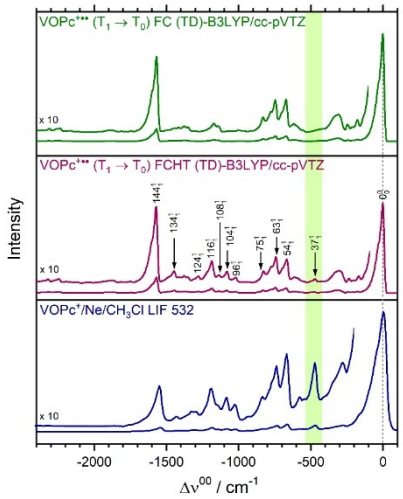


***Figure 3.*** LIF spectrum of $VOPc^{+\bullet\bullet}$ isolated in solid Ne (532 nm excitation) at 5 K in comparison with Franck–Condon (FC) and Franck–Condon/Herzberg–Teller (FCHT) TD-B3LYP/cc-pVDZ predictions. The spectra are plotted with respect to the 0-0 band origin at 11923 $cm^{-1}$—see also main text and Table S4. The green shaded area indicates the region with the significant deviation between the theory and experiment.

[1] Here "$S_0$" lies higher than "$T_1$" and therefore we switch the nomenclature to $S_1$ and $T_0$.

method improves agreement between the experimental and predicted LIF spectra. In the FCHT approximation, a linear dependence of the transition dipole moment on the nuclear coordinates is additionally considered, causing the phenomenon of intensity borrowing: the so-called Herzberg–Teller vibronic coupling effect. The HT effect is dominant in "vibronically coupled allowed" (weak) transitions and can also become important for "bright transitions" if electronic density changes noticeably with normal coordinate motion.[21] A similar effect of FC/HT interference has been reported for free-base porphyrin[22] and we have also recently pointed it out for the $H_2Pc$ and ZnPc systems.[11] Almost every vibrational mode contributing to the measured LIF spectrum of $VOPc^{+\bullet\bullet}$ shows satisfactory agreement with the calculated spectrum using the FCHT method. The only deviation is seen for mode $\nu_{37}$ (marked green in Figure 3)—involving in-plane deformation with contributions from C–C–C, C–N–C, H–C–C, and N–V–N bending. The intensity of this mode is highly underestimated by theory. The origin of this deviation has to be evaluated by more sophisticated theoretical studies. The strongest HT coupling is seen in three relatively intense features assigned as modes $\nu_{116}$, $\nu_{108}$, and $\nu_{104}$ in Figure 3.

The cryo-matrix LIF spectra discussed above show no prominent emission which can be assigned to $VOPc^{\bullet}$. While we observed an extremely weak line at 642 nm measured with 532 nm excitation (see Figure S11), this emission is blue-shifted relative to the $VOPc^{\bullet}$ absorption maximum at 658 nm thus ruling it out as the carrier. (The origin of this weak emission line is presently unclear). Note, that Huang and Sharp observed a very weak fluorescence band centered at 670–710 nm in diluted solutions of $VOPc^{\bullet}$ in dichloromethane (DCM), chloronaphthalene, and tetrahydrofuran at room temperature and assigned it to the spin-allowed $^2Q \rightarrow {}^2\Gamma$ (in Ake-Gouterman's convention[23]—equivalent to $D_{3/4} \rightarrow D_0$) transition of $VOPc^{\bullet}$.[15] In their LE-STM measurements of individual $VOPc^{\bullet}$ molecules deposited onto an Ag(111) single crystal partially covered by a NaCl bilayer, Kaiser *et al.* reported a similar weak emission line with a maximum at 680 nm.[16] No evidence for VOPc cation formation was observed in that study. Instead, positioning the tip above the O atoms of individual $VOPc^{\bullet}$ molecules resulted in their reduction to VPc and quenching of the luminescence.

To repeat the experiment of Huang and Sharp and to check for emission of $VOPc^{\bullet}$ even further to the near-infrared region, we measured photoluminescence spectra of $VOPc^{\bullet}$ in DCM solution ($\approx 10^{-6}$ M) at room temperature and 8 K—up to 1400 nm (Figure 4 and S12). Consistent with the results in Ref. [15], a sharp emission at 695 nm with a vibronic satellite at 767 nm was observed in the room temperature measurement. The corresponding excitation spectrum (PLE) tracks well with the absorption of $VOPc^{\bullet}$ in DCM (Figure S13). Note, that the prominent vibronic feature in the emission spectrum shifted by $\approx 1500\ cm^{-1}$ relative to the 0-0 transition is characteristic for Pc molecules.[24] The emission origin manifests a small Stokes of only 130 $cm^{-1}$. Its quantum yield was determined as $(1.1 \pm 0.2) \times 10^{-5}$, i.e. quite low. In contrast to the results of Huang and Sharp, practically no features attributable to the presence of $VOPc^{\bullet}$ aggregates were observed (such as an emission broadening and shoulder at ca. 660 nm).[15] Thus, the spectra in Figure 4 indicate that dilute DCM solutions at room temperature contain primarily monomeric $VOPc^{\bullet}$, with a negligible fraction of dimers and higher aggregates. Remarkably, a very weak and broad emission was also detected at 1290 nm. Its integral intensity and, accordingly, efficiency are an order of magnitude less than the already weak red emission at 695 nm. We tentatively assign this NIR band to the $D_{1/2} \rightarrow D_0$ transition (predicted for a free $VOPc^{\bullet}$ molecule at 1150 nm as vertical excitation with zero-oscillator strength—see above and Table S2).

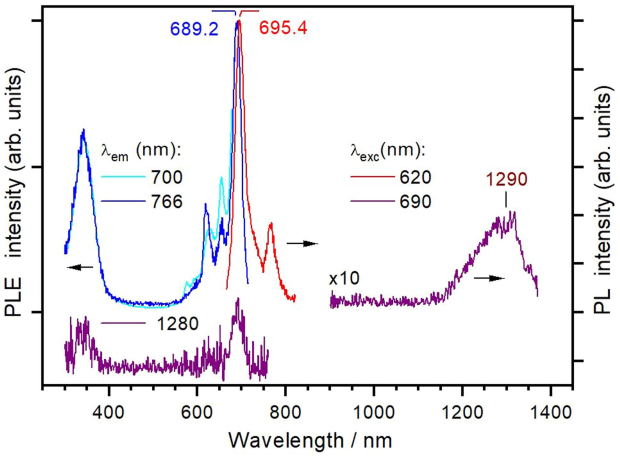


***Figure 4.*** Photoluminescence emission (PL) and excitation (PLE) spectra of VOPc dissolved in dichloromethane ($\approx 10^{-6}$ M) at room temperature. The respective excitation and emission wavelengths are indicated on the graph. The emission of $VOPc^{\bullet}$ is very weak, particularly in the NIR region (see main text), and was correspondingly recorded using large monochromator slits (5–10 nm) and long acquisition times (up to 1 h). The visible and NIR emission spectra are presented on the same intensity scale. The NIR excitation spectrum is vertically shifted for clarity.

Cooling of $VOPc^{\bullet}$ solution in DCM to its freezing point and further down to cryogenic temperatures might be expected to provide a more direct comparison with the Ne matrix measurements. However, the PL spectra of $VOPc^{\bullet}$ in DCM, cooled relatively slowly to 8 K ($\approx 1.5$ h), differ dramatically from those of monomeric $VOPc^{\bullet}$ (in DCM at room temperature) displaying a broad emission at about 900 nm (see Figure S12) characteristic for large $VOPc^{\bullet}$ aggregates.[15] Apparently, upon cooling in DCM solution, aggregation of $VOPc^{\bullet}$ becomes favorable even in the concentration range of $10^{-6}$ M. The resulting $VOPc^{\bullet}$ aggregates then dominate the PL spectra in the NIR range.

VOPc aggregation cannot occur in soft-landing (co)deposition of cations with neon under cryogenic matrix isolation conditions. Thus, the literature[15] and our DCM solution results support the conclusion, that the PL of dilute $VOPc^{\bullet}$ in Ne matrix at 5 K is too weak to be detectable under our experimental conditions. As a corollary, $VOPc^{+\bullet\bullet}$ must emit several orders of magnitude more efficiently than does $VOPc^{\bullet}$. In harnessing this strongly charge state-

dependent NIR emission of monomeric VOPc for future applications it will therefore be important to control aggregation.

## Conclusion

In summary, the vibrationally resolved absorption and LIF spectra obtained upon depositing ionized VOPc into Ne at 5 K have been recorded, assigned to a mixture of $VOPc^{\bullet}$ and $VOPc^{+\bullet\bullet}$ carriers, and compared with TD-DFT calculations using the FCHT method. A satisfactory agreement between the respective theoretical predictions and the experimental spectra obtained for $VOPc^{+\bullet\bullet}$ (absorption/LIF) and $VOPc^{\bullet}$ (absorption) allowed us to derive tentative assignments of the observed vibronic structure.

The stable neutral radical vanadyl phthalocyanine $VOPc^{\bullet}$ forms a diradical cation $VOPc^{+\bullet\bullet}$ upon electron impact ionization. This species shows profound, UV/Vis-NIR excitable photoluminescence with a band origin at 11 923 $cm^{-1}$ (839 nm) in the technologically useful NIR region.[25] By contrast, $VOPc^{\bullet}$ itself shows only negligible photoluminescence.

Over the last decades, different strategies have been applied to develop "on-off" molecular luminescence switches. To the best of our knowledge, charging the molecules has always been reflected either in luminescence annihilation (neutral molecule is the bright state, whereas the charged radical counterpart is dark)[2a] or luminescence tuning (where both neutral and charged states are fluorescent).[9,10] The only exception was the oxidation of ex-TTF-$BODIPY^{+\bullet}$ radical to ex-TTF-$BODIPY^{2+}$, where the dark radical was electrochemically transformed into the bright dication. VOPc is a rare example of a robust molecular on-off photo-switch for NIR emission, which is activated simply by ionization. This opens new possibilities for the design and development of NIR electrofluorochromism based optoelectronics. For this, further studies on the electrochemistry of VOPc and other similar molecules in diluted solutions, as well as single molecule probes on surfaces are required.

## Acknowledgements

K.A.H. is a recipient of the Humboldt Research Fellowship. The computational time was provided by the bwForCluster JUSTUS 2 at the University of Ulm. M.K. and S.D. acknowledge DFG funding via TRR 88 "3 MET" (C6). M.K. also acknowledges the support of instrumental infrastructure by the Helmholtz Research Field "Information". Open Access funding enabled and organized by Projekt DEAL.

## Conflict of Interest

The authors declare no conflict of interest.

## Data Availability Statement

The data that support the findings of this study are available from the corresponding author upon reasonable request.

**Keywords:** Biradical Cation · Luminescence · Matrix Isolation · Photo-Switch · Vanadyl Phthalocyanine

[1] a) P. Audebert, F. Miomandre, *Chem. Sci.* **2013**, *4*, 575–584; b) M. H. Chua, Q. Zhu, K. W. Shah, J. Xu, *Polymer* **2019**, *11*, 98.
[2] a) M. Čížková, L. Cattiaux, J.-M. Mallet, E. Labbé, O. Buriez, *Electrochim. Acta* **2018**, *260*, 589–597; b) C. D. Geddes, J. R. Lakowicz, *Advanced concepts in fluorescence sensing: Part A: Small molecule sensing, Vol. 9*, Springer Science & Business Media, Cham, **2007**.
[3] A. B. Scharf, S.-L. Zheng, T. A. Betley, *Dalton Trans.* **2021**, *50*, 6418–6422.
[4] Z. Cui, A. Abdurahman, X. Ai, F. Li, *CCS Chem.* **2020**, *2*, 1129–1145.
[5] M. Abe, *Chem. Rev.* **2013**, *113*, 7011–7088.
[6] N. L. Bill, J. M. Lim, C. M. Davis, S. Bähring, J. O. Jeppesen, D. Kim, J. L. Sessler, *Chem. Commun.* **2014**, *50*, 6758–6761.
[7] H. Namai, H. Ikeda, Y. Hoshi, N. Kato, Y. Morishita, K. Mizuno, *J. Am. Chem. Soc.* **2007**, *129*, 9032–9036.
[8] a) A. Zampetti, A. Minotto, F. Cacialli, *Adv. Funct. Mater.* **2019**, *29*, 1807623; b) W. Jiang, X. Chen, T. Wang, B. Li, M. Zeng, J. Yang, N. Hu, Y. Su, Z. Zhou, Z. Yang, *RSC Adv.* **2021**, *11*, 5618–5628; c) N. Chaulagain, K. M. Alam, P. Kumar, A. E. Kobryn, S. Gusarov, K. Shankar, *Nanotechnology* **2022**, *33*, 055703; d) J. Liu, K. Luo, H. Chang, B. Sun, Z. Wu, *Nanomaterials* **2021**, *11*, 2713; e) X. Zhang, C. Wolf, Y. Wang, H. Aubin, T. Bilgeri, P. Willke, A. J. Heinrich, T. Choi, *Nat. Chem.* **2022**, *14*, 59–65; f) K. Prabhu, C. P. M. Nemakal, M. Managa, T. Nyokong, L. Koodlur Sannegowda, *Front. Chem.* **2021**, *9*, 452.
[9] V. Rai, L. Gerhard, Q. Sun, C. Holzer, T. Repän, M. Krstić, L. Yang, M. Wegener, C. Rockstuhl, W. Wulfhekel, *Nano Lett.* **2020**, *20*, 7600–7605.
[10] B. Doppagne, M. C. Chong, H. Bulou, A. Boeglin, F. Scheurer, G. Schull, *Science* **2018**, *361*, 251–255.
[11] K. A. Haupa, N. P. Krappel, D. Strelnikov, M. M. Kappes, *J. Phys. Chem. A* **2022**, *126*, 593–599.
[12] a) B. Kern, D. Strelnikov, P. Weis, A. Böttcher, M. M. Kappes, *J. Phys. Chem. A* **2013**, *117*, 8251–8255; b) B. Kern, D. Strelnikov, P. Weis, A. Böttcher, M. M. Kappes, *J. Phys. Chem. Lett.* **2014**, *5*, 457–460; c) D. V. Strelnikov, B. Kern, M. M. Kappes, *J. Phys. Chem. A* **2017**, *121*, 7356–7361.
[13] M. Sato, T. Kwan, *J. Chem. Phys.* **1969**, *50*, 558–559.
[14] a) R. Aroca, R. O. Loutfy, *Spectrochim. Acta Part A* **1983**, *39*, 847–852; b) P. Kivits, R. De Bont, J. Van der Veen, *Appl. Phys. A* **1981**, *26*, 101–105; c) I. Cimatti, L. Bondi, G. Serrano, L. Malavolti, B. Cortigiani, E. Velez-Fort, D. Betto, A. Ouerghi, N. Brookes, S. Loth, *Nanoscale Horiz.* **2019**, *4*, 1202–1210; d) L. Guo, G. Ma, Y. Liu, J. Mi, S. Qian, L. Qiu, *Appl. Phys. B* **2002**, *74*, 253–257; e) M. R. Kiran, H. Ulla, M. Satyanarayan, G. Umesh, *Opt. Mater.* **2019**, *96*, 109348; f) J. Zhang, Z. Wang, T. Niu, Z. Li, W. Chen, *Appl. Phys. Lett.* **2014**, *104*, 113506; g) Y. Tamaki, T. Asahi, H. Masuhara, *Jpn. J. Appl. Phys.* **2003**, *42*, 2725; h) Y. Pan, Y. Wu, L. Chen, Y. Zhao, Y. Shen, F. Li, S. Shen, D. Huang, *Appl. Phys. A* **1998**, *66*, 569–574.
[15] T. Huang, J. Sharp, *Chem. Phys.* **1982**, *65*, 205–216.
[16] K. Kaiser, L. Gross, F. Schulz, *ACS Nano* **2019**, *13*, 6947–6954.

[17] D. V. Strelnikov, M. Link, J. Weippert, M. M. Kappes, *J. Phys. Chem. A* **2019**, *123*, 5325–5333.
[18] P. Vincett, E. Voigt, K. Rieckhoff, *J. Chem. Phys.* **1971**, *55*, 4131–4140.
[19] K. A. Haupa, A. Szukalski, J. Myśliwiec, *J. Phys. Chem. A* **2018**, *122*, 7808–7818.
[20] M. Kasha, *Discuss. Faraday Soc.* **1950**, *9*, 14–19.
[21] R. Improta, V. Barone, F. Santoro, *J. Phys. Chem. B* **2007**, *111*, 14080–14082.
[22] F. Santoro, A. Lami, R. Improta, J. Bloino, V. Barone, *J. Chem. Phys.* **2008**, *128*, 224311.
[23] R. L. Ake, M. Gouterman, *Theor. Chim. Acta* **1969**, *15*, 20–42.
[24] C. Murray, N. Dozova, J. G. McCaffrey, N. Shafizadeh, W. Chin, M. Broquier, C. Crépin, *Phys. Chem. Chem. Phys.* **2011**, *13*, 17543–17554.
[25] Y. Cai, Z. Wei, C. Song, C. Tang, W. Han, X. Dong, *Chem. Soc. Rev.* **2019**, *48*, 22–37.

Manuscript received: January 28, 2022
Accepted manuscript online: March 29, 2022
Version of record online: April 21, 2022